Archives of Hydro-Engineering and Environmental Mechanics 69 (2022), pp. 27–43, doi: 10.2478/heem-2022-0003

sciendo

ARCHIVES OF HYDRO-ENGINEERING AND ENVIRONMENTAL MECHANICS

Published since 1954 ISSN 1231–3726

Numerical Modeling of Compound Channels for Determining Kinetic Energy and Momentum Correction Coefficients Using the OpenFOAM Software

Nariman Mehranfar[1], **Elham Ghanbari-Adivi**[2]

[1] Department of Civil Engineering, Amirkabir University of Technology,Tehran, Iran;
[2] Department of Water Science Engineering, Shahrekord University, Shahrekord, Iran,
Corresponding author: e-mail: ghanbariadivi@sku.ac.ir

(Received 07 September 2021; revised 02 May 2022)

Abstract. The non-uniformity of the flow velocity distribution in each section of compound channels and in the main channel-floodplain interface area causes errors in estimating water surface profile, flood routing, pollution transfer, and so on. To reduce the impacts of non-uniformity on the exact calculation of kinetic energy and momentum, α and β correction coefficients are used, respectively. However, the determination method of these coefficients is a challenging issue in river engineering. This study used the OpenFOAM Software to determine these coefficients numerically for two laboratory models of compound open channels of which the data are available, using the single-phase pimpleFoam solver to do modeling in the mentioned software and the k-ωSST turbulence model to calculate the flow characteristics. Based on the results, the highest difference (13%) between the results estimated by the software and those obtained from the lab experiments was seen in the low flow depth where the flow left the main channel and entered the floodplain of a very shallow depth, possibly due to the grid generation of this area. This difference decreased as the flow depth increased, and its average was 6.65% for α coefficient and 2.32% for β coefficient in all cases, which means the results of numerical modeling and the experimental data conformed well, and the OpenFOAM software can be successfully used in flow modeling and analyzing flow characteristics in compound channels.

Key words: Compound channel, floodplain, OpenFOAM, SST turbulence model, correction coefficients, kinetic energy, momentum

List of Abbreviations

CES – Conveyance Estimate System
CFD – Computational Fluid Dynamics
DES – Detached-Eddy Simulation
FCF – Flood Channel Facility
HEC-RAS – Hydrologic Engineering Center's – River Analysis System

LES – Large Eddy Simulation
OpenFOAM – Open Field Operation And Manipulation
PIMPLE – merged PISO-SIMPLE)
PISO – Pressure Implicit with Splitting of Operator
RAS – Reynolds-Averaged Stress
RANS – Reynolds Averaged Navier-Stokes
SIMPLE – Semi-Implicit Method for Pressure-Linked Equations
SST – Shear Stress Transport

1. Introduction

The non-uniformity of velocity distribution in the main channel-floodplain interface area in compound channels (Shiono and Rameshwaran 2015, Mohanty and Khatua 2014, Al-Khatib et al 2013, Fernandes 2013, French 1987, Knight et al 1984) creates turbulences, vortices and shear forces in the interface area, which leads to the dissipation of flow energy and reduced flow transfer capacity (Fernandes et al 2015). Due to the velocity deviation from the theory of uniform velocity distribution in compound channels, the measurement of kinetic energy and momentum is challenging and requires correction coefficients known as α coefficient (Coriolis 1836) and β coefficient (Boussinesq 1877), respectively. No correction coefficients are needed when transverse and deep velocity distributions are uniform in the channel section ($\alpha = \beta = 1$). The non-uniform velocity distribution in compound channels is affected by factors such as channel slope, cross-section shape, curvature, and bed roughness and flow depth (Chow 1951, French 1987). As the kinetic energy and momentum correction coefficients are highly affected by rigid boundaries, especially in compound channels with varying geometries, their inaccurate measurement will cause erroneous assessment of flow behavior, afflux, discharge scale, and so on. Although predetermined α and β values can be used in natural channels, for reducing structure design errors, these coefficients should be accurately determined in compound sections consisting of a deep main channel with a fast flow surrounded by one or two floodplains with shallow and slow flows.

Several one-dimensional models, such as ISIS, HEC-RAS, and MIKE 11 have been used for studying flow characteristics and determining α and β values; however, they have unphysical bases, need boundary resistance coefficients, overestimate floodplains, and underestimate main channels (Ghanbari-Adivi 2020).

Also, some calculations of quasi-2D were found to be inaccurate for the interface zone because the secondary flow, friction factor, and eddy viscosity were uncertain. So, these models should include correction coefficients, specifically near shear layers.

The poor performance of 1D and quasi-2D models in analyzing flows in complex conditions such as compound channels and main channel-floodplain interface areas has drawn attention to 2D/3D models, which can improve the accuracy of estimated

results by the cell by cell study of the phenomenon instead of averaging the parameters.

Numerical simulation of turbulent flows by Navier-Stokes equations requires the analysis of a wide range of spatial and temporal scales. Direct numerical simulation provides accurate results of the flow by on all spatial and temporal scales (Sagaut 2006).

OpenFOAM is free, open-source software that has attracted the attention of many researchers in recent years. It is capable of parallelizing a large volume of data analyses and solving Navier-Stokes equations by the finite volume method, which is based on dividing the computational domain into small non-intersecting multidimensional domains called "control volume". In OpenFOAM, all variables are first stored in the center of the control volume and then attributed to the entire body. The pimpleFoam solver has been designed and implemented in OpenFOAM to solve filtered Navier-Stokes equations.

Using a combined staggered-collocated grid approach, the OpenFOAM stores both the velocity and pressure in its center, but carries out the velocity computations in faces as a flux. It first treats the flux as a primary variable over velocity to maintain velocity coupling with pressure and then reforms it for use in momentum equations (Rusche 2002).

The pressure-based, segregated pimpleFOAM solver uses implicit discretization. Its velocity-pressure coupling technique comprises a momentum predictor for previous pressure field-based velocity field, a pressure-field correction Poisson solver, and a momentum corrector (Rusche 2002). The algorithm used in this solver is based on a combination of SIMPLE and PISO transient algorithms, which enables it to analyze various behaviors from different flows and apply a variety of turbulence modeling methods (Versteeg and Malalasekera 2007, Piomelli 1993). PISO, used for time-dependent flows, first neglects velocity corrections and performs more pressure corrections, and SIMPLE, used for steady state problems, has a pressure correction term and neglects velocity corrections resulting in a slow convergence (Penttinen et al 2011). The PIMPLE algorithm is a variant of the PISO, where an outer correction loop cycling over a given time step for a number of iterations and equation under-relaxation between outer correctors are allowed for stability (Rusche 2002). At the beginning of each time step, the OpenFOAM algorithm increases the simulation time until it reaches the desired time step. Then the algorithm performs the pressure-velocity loop for the coupled equations. The momentum equation is solved inside this loop and then begins the correction loop inside which the pressure equation is solved, and the velocity field is modified until reaching the continuity conditions ($\nabla V = 0$). The first loop is finally finished after the turbulence modeling-related equations are solved. In OpenFOAM, it is possible to set the number of executions for pressure-velocity coupled equations (Zahiri and Roohi 2019).

This study used the OpenFOAM software for simulating compound channels for the first time. Modeling compound channels is a challenging task because of the com-

plexity of their conditions (due to the difference in the flow condition between the main channel and floodplain). Choosing the correct modeling method is important in solving divergence and convergence and in increasing the result precision.

The geometry of the floodplain causes a smaller flow structure and calculation network and, therefore, higher calculation fees which can be reduced by choosing the correct turbulence model. Here, compound channels were simulated by the RANS (k-ωSST model).

This study also examined the effects of different flow depths on the α and β coefficients in a symmetrical compound channel and compared the results with the previous experimental data from the Flow Channel Facility (FCF). In other words, the verification of the accuracy of the employed software and the accuracy of the underlying theoretical turbulence model against laboratory data was investigated.

2. Materials and Methods

2.1. Specifications of the Laboratory Compound Channel

Data of the compound channel used for modeling different flow depths were obtained from the Wallingford Hydraulic Research Institute. The selected data belonged to series 02 and 10 symmetrical channels of 60 m long and 10 m wide.

The FCF data included flow hydraulic characteristics (discharge, total area, area of each sub-section, average velocity of each section/sub-section) and channel characteristics (bed width/slope, wall slope, floodplain width) shown in Figure 1 and Table 1.

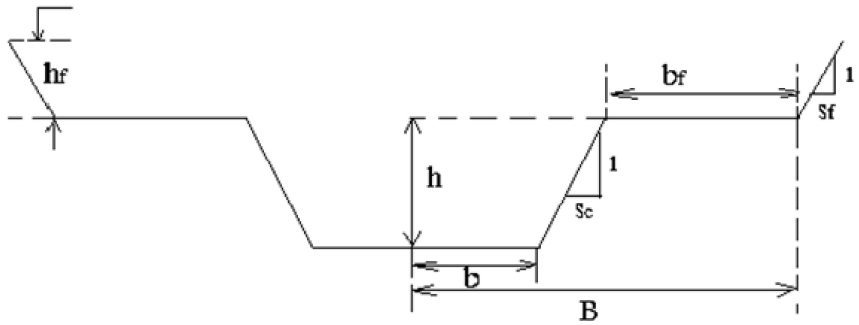

Fig. 1. The cross-section of FCF series (02 and 10) h – main channel depth; h_f – floodplain depth; B – half of main channel width; b_f – floodplain width; H – main channel flow depth; S_f – floodplain wall slope; S_c main channel wall slope

Table 1. The FCF series information

Cross section Shape	S_c	S_f	B	b_r	b	h	h_f	Series
Symmetric	1	1	3.15	2.25	0.75	0.15	0.25	02
Symmetric	2	1	3.3	2.25	0.75	0.15	0.25	10

2.2. Numerical Modeling and Procedures

2.2.1. Governing Equations

2.2.1.1. Flow equations

Ignoring water level variations, this study used the pimpleFOAM solver to model in OpenFOAM (here X, Y, Z: streamwise, vertical and cross-stream coordinates, respectively). It operates based on the continuity and momentum equations as follows:

$$\nabla u = 0, \tag{1}$$

$$\frac{\partial u}{\partial t} + \nabla \cdot (uu) = -\nabla p + \nabla T + f, \tag{2}$$

where u is the velocity vector, p is pressure, T is a deviatoric stress tensor defined as follows for incompressible flows:

$$T = 2\vartheta S, \tag{3}$$

where ϑ is viscosity and S is the mean rate of strain tensor defined as follows:

$$S = 0.5\left[\nabla u + (\nabla u)^T\right]. \tag{4}$$

The stress term in Eq. (4) for the incompressible Newtonian fluid can be defined as follows with the help of the divergence operation in vector calculus:

$$\nabla \cdot T = \nabla \cdot (\vartheta \nabla u) + \nabla u \cdot \nabla \vartheta. \tag{5}$$

In Eq. (2), f is the external force that can also include the gravity force. The mass transfer equation (2) can be rewritten, using Eq. (5), as follows:

$$\frac{\partial u}{\partial t} + \nabla \cdot (uu) - \nabla \cdot (v \nabla u) - \nabla u \cdot \nabla v = -\nabla p + f. \tag{6}$$

Finally, the flow field can be solved using Eqs. (6) (momentum) and (1) (continuity) (OpenFOAM, 2018).

2.2.1.2. Turbulence equations

The OpenFOAM software was used for numerically simulating the 3D flow in a compound channel. It works based on CFD codes written in the C^{++} language. Among its numerous models and solvers for modeling fluid dynamics problems, the

pimpleFoam solver and the three turbulence models of laminar, RAS, and LES were chosen in this study.

Reviewing the literature on open channels (Penttinen 2011, Menter et al 2003, Rusche 2002, Manokaran et al 2020), the authors decided to use the one of the two-equation turbulence models, k-ωSST model of the RAS group to simulate near-wall flows and various flow depths, selected the pressure implicit splitting operation algorithm to solve the velocity-pressure coupling, used the Gauss linear method to discretize the momentum term, fixed 0.5 (Rusche 2002) as the maximum Courant number, and used 20 parallel processors to run each program considering the high volume of calculations The two-equation turbulence model first presented by Kolmogorov in 1942 had an equation for k and one for ω and showed the energy dissipation rate/unit volume and time. Later, Saffman in 1970 proposed another k–ω model in which ω was a frequency characteristic of the turbulence decay process (Warner et al 2005).

These equations, known as k (Turbulent Kinetic Energy) and ω (specific dissipation rate of k) equations, respectively, were derived for high-Reynolds flows in which S is found by Eq. (4), F1 is a blending function, υt: kinematic turbulent viscosity, σ_ω and σ_k: model constants (Schmidt's number in υt and k equation, respectively), U is temporal average velocity tensor. $\widetilde{p_k}$ (Production of kinetic energy) was defined in Stagnation regions to prevent creating turbulence parameters. The above-mentioned constant coefficients were presented in Table 2.

Table 2. Constant coefficients of k–ωSST model

β^*	α_1	β_1	σ_{k1}	$\sigma_{\omega1}$	α_2	β_2	σ_{k2}	$\sigma_{\omega2}$
0.09	5.9	3.40	0.85	0.5	0.44	0.0828	1	0.856

Again, after the failure of most two-equation models, Menter (1993) designed a k–ωSST turbulence model that could predict adverse pressure gradient flows (Hellsten 1998). As k–ω was more accurate than $k-\varepsilon$ in near-wall layers, it performed well when flows had moderate adverse pressure gradient; however, it failed when the flow had pressure-induced separation (Menter 2009). This equation was also highly sensitive to the ω values in freestream that was outside the boundary layer (Menter 1992).

As the modeling geometry was complex (i.e., the existence of a low-height part in the floodplain and high depth parts in the main channel, which results in a free flow), the k–ωSST model was used here for correct calculating of the turbulence viscosity. First developed by Menter (1992), the k–ωSST turbulence equations use the k–ω model advantages for near walls and in boundary layers and the $k-\varepsilon$ model advantages for free flows (Penttinen et al 2011, An and Fung 2018). These two models are combined with the help of a blending function to represent the turbulence kinetic energy and specific dissipation rate as follows:

$$\frac{\partial(k)}{\partial t} + \nabla \cdot (Uk) = \nabla \cdot [(\vartheta + \sigma_k \vartheta_t) \nabla k] + \widetilde{p_k} - \beta^* k\omega, \tag{7}$$

$$\frac{\partial(\omega)}{\partial t} + \nabla \cdot (U\omega) = \nabla \cdot [(\vartheta + \sigma_\omega \vartheta_t) \nabla \omega] + \alpha S^2 - \beta\omega^2 + 2(1 - F_1)\sigma_{\omega 2} \frac{1}{\omega} (\nabla k)(\nabla \omega). \tag{8}$$

Correcting the constant values and having turbulent cross-diffusion term in ω equation, the k–ωSST model is a more precise and reliable method for a wide range of flows than the k–ω model.

2.2.2. Numerical Modeling

2.2.2.1. Boundary Conditions

For achieving reality-conforming modeling, sensitivity analysis was performed for different boundary conditions. To achieve reality-conforming modeling, sensitivity analysis was performed for different boundary conditions. Nearly all boundary conditions led to nonphysical results (for example, velocities being equal to 200 m/s, or highly oscillatory velocities occurring along the channel), except for one case that led to an acceptable physical result and was therefore considered as the proper boundary condition.

2.2.2.2. Solution Control

The initial settings included the start time, end time, and time step for the solution output. For an appropriate time step and a suitable numerical stability during the processing, the Courant Number (Eq. 9) needs to be less than one.

$$C_0 = U_c \cdot \frac{\Delta t}{\Delta x}, \tag{9}$$

where C_0 is the Courant Number, U_c is the cell velocity, Δx is the cell size in the direction of the velocity, and Δt is the time step. The cell size is found as follows:

$$\Delta x = \frac{d}{n}, \tag{10}$$

where d is the channel length in the direction of the velocity and n is the number of cells created along the channel.

3. Results and Discussion

3.1. Sensitivity Analysis

For creating the geometry and its grids, blockMesh in the OpenFOAM Software was used. The geometry grid was structured, which means the cell dimensions were uniform in a cross-section, except in the boundary layer in which they had an expansion

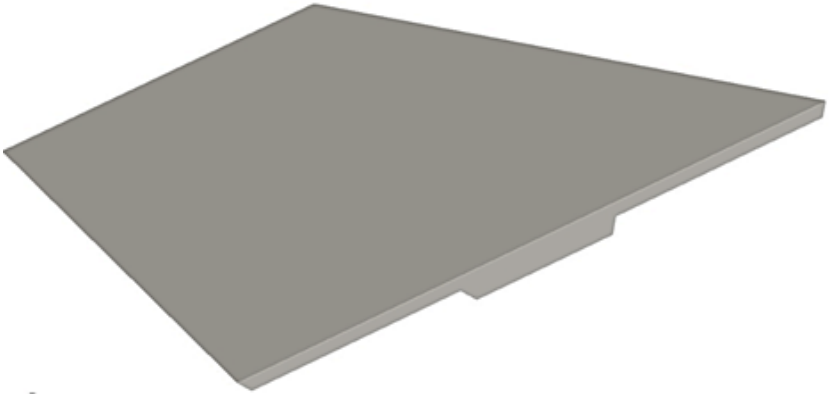

Fig. 2. General view of the modeling geometry

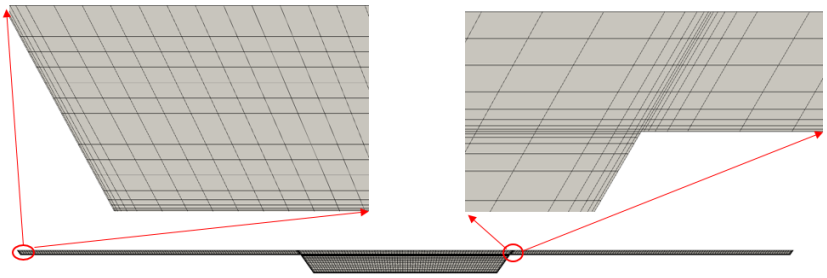

Fig. 3. Cross-sectional grid generation

ratio near the walls. The cells were small near the walls but became greater as departing from the wall until reaching the uniform size (Figures 2 and 3).

It was assumed that the grid generation was uniform along the channel, and the grid size along the channel was equal to that across the channel. For selecting the size, different grids were tested, and the values of α and β were determined for each cell size. The best size was then selected by analyzing the related graph (Figure 4).

As shown, the grid size of < 0.01 m could be considered for all models, as α and β values remained unchanged in that size. For grid generation of the boundary layer, a dimensionless distance from reference value of y^+, proportional to the mean friction velocity (u_τ), was used ($y^+ = (y \cdot u_\tau)/\vartheta) \cdot y^+$ is an important parameter to be considered in any CFD simulation for achieving good results. It was calculated separately for each simulation, which means the data drawn for an equal value of y^+ lay in different spatial positions (y). The result of the k–ωSST turbulence model is closer to reality when $y^+ < 10$ (Menter et al 2003); hence, this value was considered in all models. Here, the maximum value of y^+ is 8.16 (< 10).

The desired geometry was meshed through the Python program by which the coordinates of points were extracted for blockMesh using the Python codes. The number

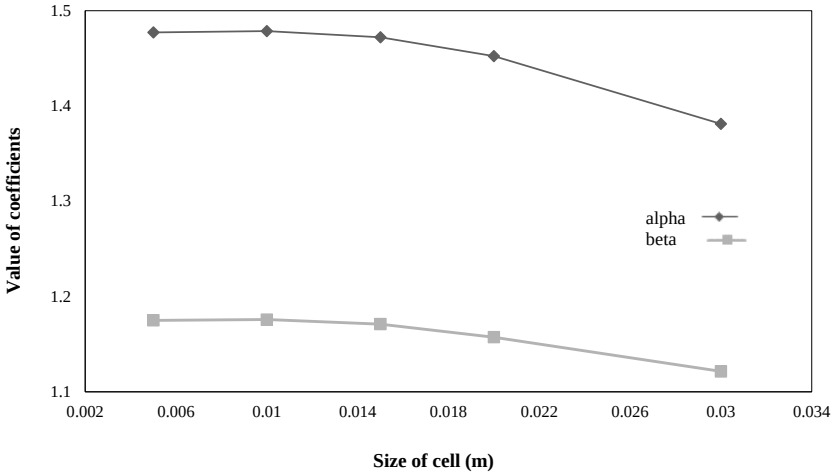

Fig. 4. Cell size sensitivity analysis

of meshes was determined based on the distance, and the number of meshes in the boundary layer was calculated based on the aspect ratio. To study the flow status in compound sections, 18 different modes, each with a mean run-time of 60 h (totally 1080 h), were examined. Averagely, about 2 million cells were created for each model, which required a strong processing system as the following:
ryzen 3900x 12 core 24 thread 32 gb, RAM 250 gb, hard ssd nvme 2 TB hard hdd system.

3.2. Fully Developed Flow Region

To obtain output from the results and determine α and β, the length of fully developed flow region was found as follows (White 1999):

$$\frac{\delta}{L} = \frac{5}{Re^{0.5}} \quad 10^3 < Re < 10^6, \tag{11}$$

where δ is the thickness at the edge of the outer boundary layer ($\delta = y$), L is the developed length (part of flow channel length), and Re is the Reynolds number. After finding the developed length, α and β values were calculated for several sections along the channel.

As shown, as the ratio of the distance of the desired point (L_0) to the developed length (L) increased towards one, α and β values tended to remain unchanged. According to the figure (5), the geometry length can be considered equal to the developed length and the output results as the solution; however, the modeling lengths were taken 1.2 times the developed length to reduce errors. Table 3 lists, as an example, the model output results for the series 2 channel at different depths for different flow discharge (Q) with certain magnitude velocity (U).

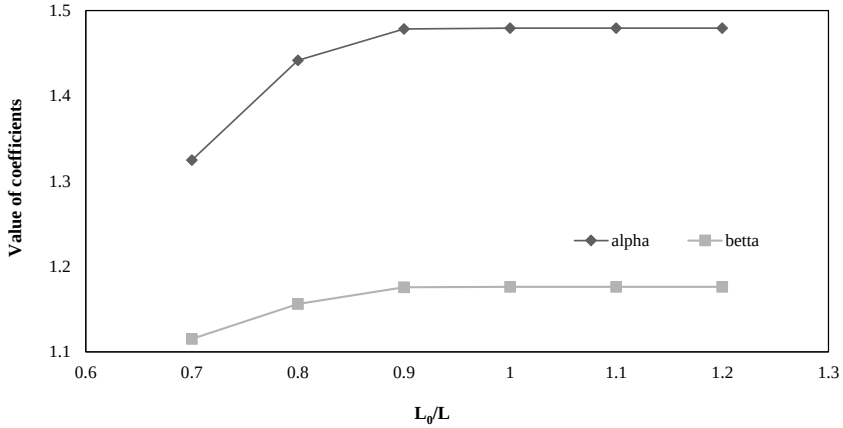

Fig. 5. Values of α and β for different distances from the inlet (H = 0.1687 m)

Table 3. Developed lengths in series 02 channel at different flow depths

H (m)	δ (m)	Re	Total cell	y^+(max)	Q(m^3/s)	U (m/s)	Time (s)	L (m)
0.1565	0.2213	166686		8.168	0.212	0.753	80	19
0.1687	0.2386	165026		8.136	0.248	0.692	90	20
0.1699	0.2403	163347		7.938	0.249	0.680	90	20
0.1778	0.2514	170269		9.461	0.282	0.677	100	21
0.1868	0.2642	180520	5503120	7.965	0.324	0.683	100	23
0.1870	0.2645	180296		8.544	0.324	0.682	100	23
0.1980	0.2800	196905		8.325	0.383	0.703	110	25
0.2136	0.3021	224993		7.126	0.480	0.745	120	29
0.2486	0.3516	308701		8.133	0.763	0.878	140	40
0.2880	0.4073	403823		9.123	1.114	0.991	160	52

3.3. Velocity Contours in the Channel

The OpenFoam output (Figures 6–8) shows changes in velocities in all three dimensions due to changing section area (increased flow depth) and developing flow turbulence. The generated turbulence and secondary flow especially in the interface between the main channel and floodplain affect the velocity and its distribution. Therefore, study of changes in three dimensions and calculating the resulting velocity is necessary for the exact calculation of the energy and momentum of flow. The modeling performed by Openfoam in this study helped in calculating the velocity and then the area of each cell (using ParaView) and related coefficients with an acceptable precision (discussed in 3.3). The velocity contours for different depths in different directions (X, Y, Z: streamwise, vertical and cross-stream coordinates) in terms of meters and the velocity magnitude (U: m/s), for channel series 2 are presented in Figures 6–9.

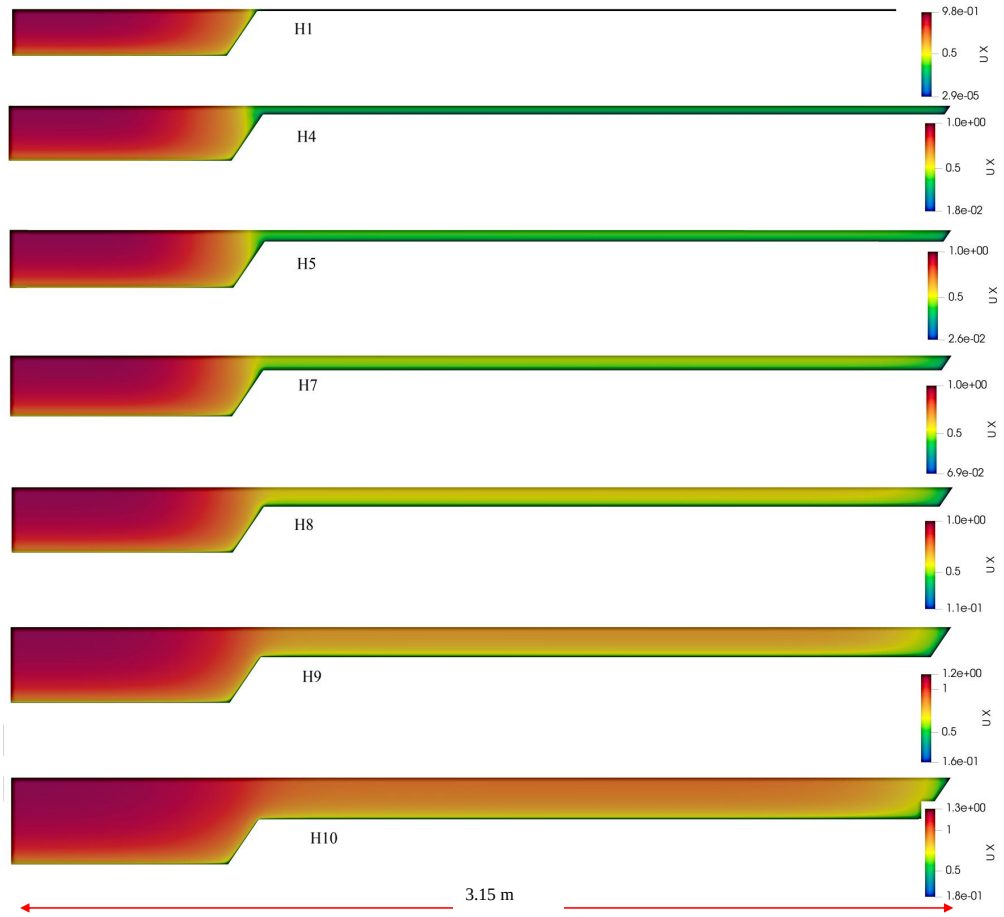

Fig. 6. Velocity (m/s) contours along the X axis, for different height of flow (H1 – H10)

3.4. Determining the Kinetic Energy and Momentum Correction Coefficients

The software determined the velocity in each cell by calculating its magnitude in all three dimensions and then, using Paraview, calculated the area to find the coefficients based on the defined relations.

The results were then compared with actual data (Figures 10–11) for assessing the performance of the Software in modeling the flow in compound sections (Section 3–4).

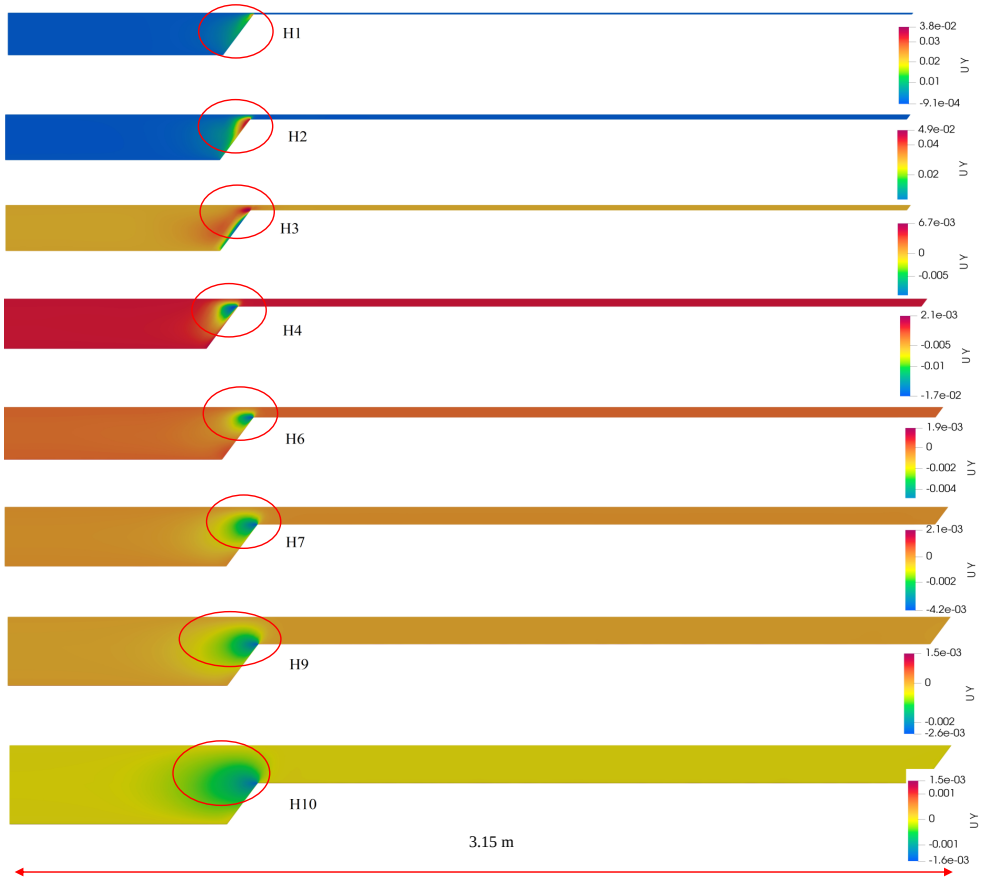

Fig. 7. Velocity (m/s) contours along the Y axis, for different height of flow (H1 – H10)

3.5. Calculating the Difference Between the Model and Actual Results for α and β

The difference between the actual and OpenFOAM results was calculated for each coefficient for each channel (Table 4 and 5).

The results showed that the highest difference (13%) belonged to the α value in channel 02. The difference between the experimental and software results increased when the floodplain flow was shallow because the mesh size variations complicated the geometry, which questioned the accuracy of the modeling. The increase in the channel flow depth, on the other hand, reduced the difference between the results. In both channels, the highest model-lab result conformity occurred in the 0.21–0.24 m depth range. Here the SST model overestimates the velocity in the compound channel.

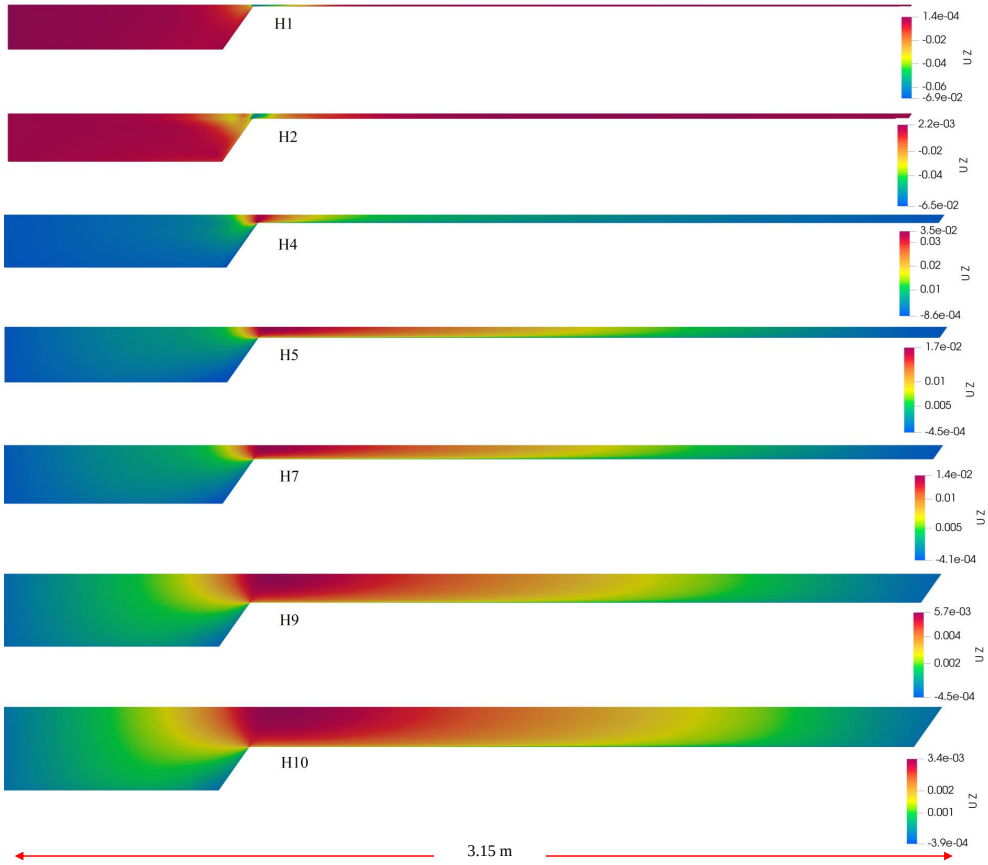

Fig. 8. Velocity (m/s) contours along the Z axis, for different height of flow (H1 – H10)

4. Conclusions

This study used the pimpleFOAM solver and turbulence equations in the single-phase mode to model the flow in compound channels. The model outputs showed that the

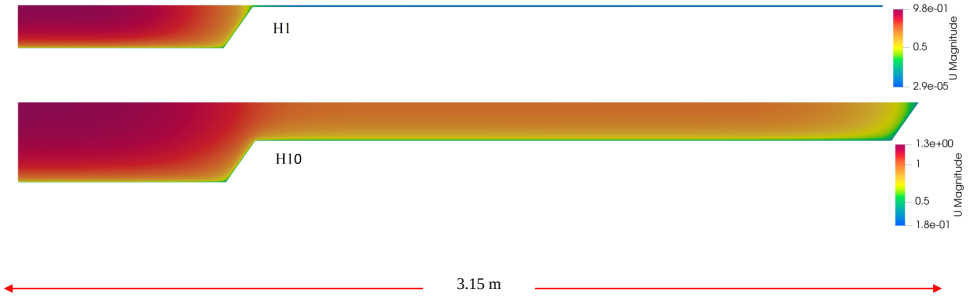

Fig. 9. Magnitude velocity (m/s) contours for different height of flow (H1 and H10)

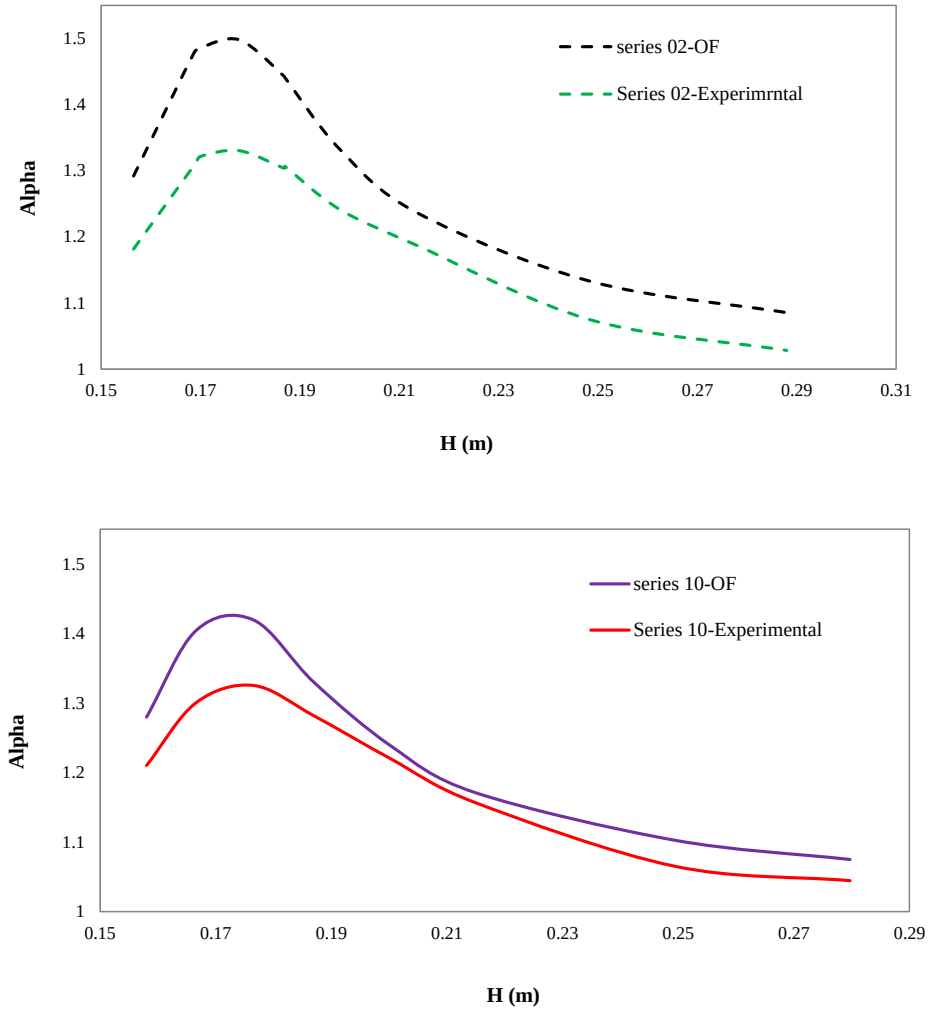

Fig. 10. Values of α in different channel flow depths

experimental and model results agreed well. The most difference occurred when the flow was shallow on the floodplain, and the least occurred when the flow depth was considerable.

Therefore, OpenFOAM can be strongly recommended in modeling free flows in compound sections. The accuracy of the results highly depends on the geometry and its meshing. More studies including two-phase studies and the use of other solvers are needed for future modeling of the compound channels.

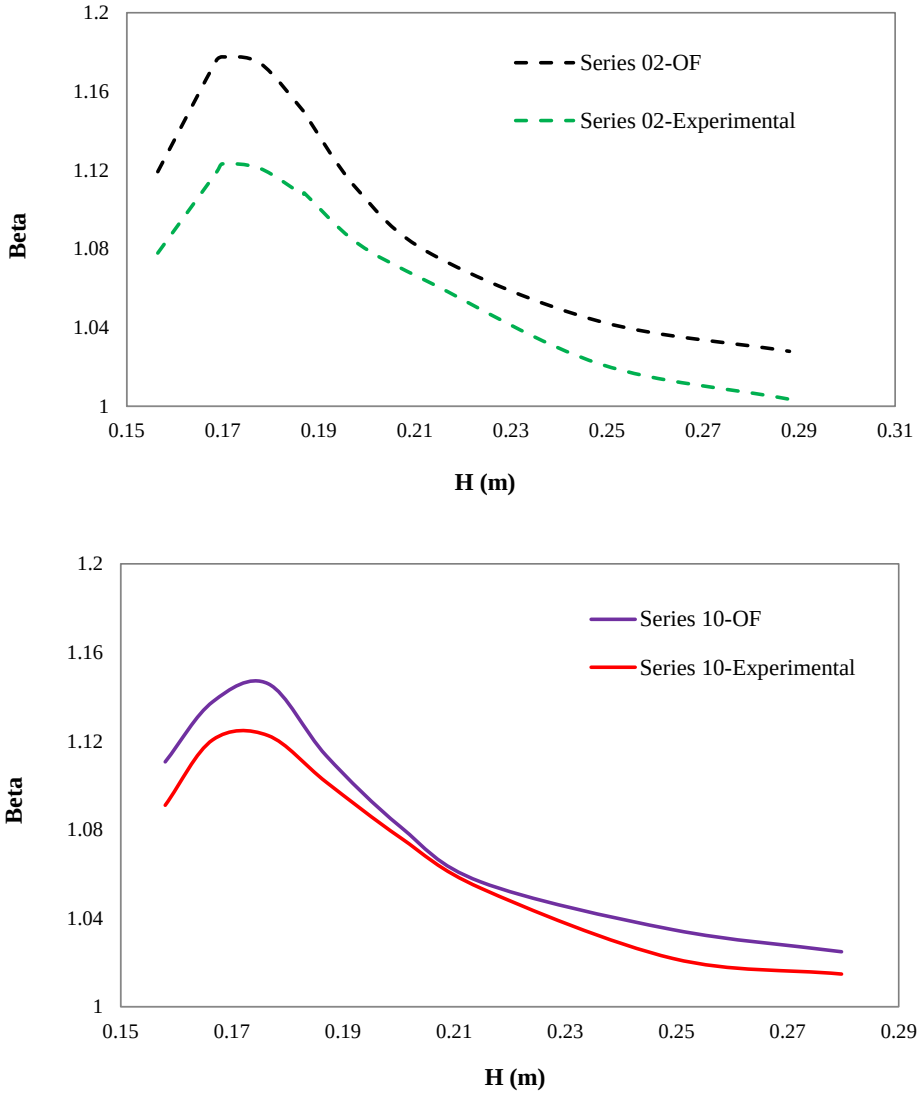

Fig. 11. Values of β in different channel flow depths

Declaration of competing interest

The authors declare that they have no known competing financial interests or personal relationships that could have appeared to influence the work reported in this paper.

Table 4. Percent difference between measured and OpenFOAM results for α and β in different depths (series 02)

H (m)	α Difference (%)	β Difference (%)
0.1565	9.36	3.84
0.1687	13.04	5.09
0.1699	12.44	4.85
0.1778	12.62	4.78
0.1868	10.69	3.85
0.1870	10.29	3.69
0.1980	7.36	2.52
0.2136	4.17	1.40
0.2486	5.43	2.11
0.2880	5.57	2.42
Average	9.10	3.45

Table 5. Percent difference between measured and OpenFOAM results for α and β in different depths (series 10)

H (m)	α Difference (%)	β Difference (%)
0.15803	5.75	1.80
0.1666	7.98	1.54
0.17654	7.09	2.09
0.18701	3.73	1.09
0.20033	1.51	0.46
0.21481	1.23	0.27
0.2493	3.51	1.27
0.2797	2.92	0.99
Average	4.22	1.19

Acknowledgments

This study was funded by the University of Shahrekord, Iran. The financial support of this organization is appreciated (GN: 141/5328). Also, we thank the Wallingford-HR Institute for providing and sharing the data that was used in this research.

References

Al-Khatib I. A., Abu-Hassan H. M. Abaza K. A. (2013) Development of empirical regression-based models for predicting mean velocities in asymmetric compound channels, *Flow Measurement and Instrumentation*, **33**, 77–87.

An K., Fung J. C. H. (2018) An improved SST $k-\omega$ model for pollutant dispersion simulations within an isothermal boundary layer, *Journal of Wind Engineering and Industrial Aerodynamics*, **179**, 369–384.

Boussinesq J. (1877) *On the theory of flowing waters*, Paris.

Chow V. T. (1951) *Open-Channel Hydraulics*, McGrawHill, New York.

Coriolis G. (1836) On the Backwater-curve equation and the corrections to bBe introduced to account for the difference of the velocities at different points on the same cross section, *Annales des Ponts et Chaussées*, **11** (1), 314–335.

Fernandes J. N. (2013) Compound channel uniform and non-uniform flows with and without vegetation in the floodplain, *Doctoral dissertation*.

French R. H. (1987) *Open-Channel Hydraulics*, McGrawHill, Singapore, 2nd edition.

Ghanbari-Adivi E. (2020) Compound Channel's Cross-section Shape Effects on the Kinetic Energy and Momentum Correction Coefficients, *Archives of Hydro-Engineering and Environmental Mechanics*, **67** (1–4), 55–71, https://doi.org/10.1515/heem-2020-0004.

Hellsten A. (1998) Some improvements in Menter's k-omega SST turbulence model, *29th AIAA, Fluid Dynamics Conference*, p. 2554.

Knight D. W., Demetriou J. D., Hamed M. E. (1984) Stage discharge relationships for compound channels, [In:] Smith KVH (ed) *Channels and channel control structures*, Springer, Berlin, pp. 445–459.

Manokaran K., Ramakrishna M., Jayachandran T. (2020) Application of flux vector splitting methods with SST turbulence model to wall-bounded flows, *Computers & Fluids*, **208**, p. 104611, https://doi.org/10.1016/j.compfluid.2020.104611.

Menter F. R. (1992) Influence of freestream values on $k - \omega$ turbulence model predictions, *AIAA Journal*, **30** (6), 1657–1659.

Menter F. R. (1993) Zonal two-equation $k - \omega$ turbulence model for aerodynamic flows, *AIAA Paper 1993-2906*.

Menter F. R. (2009) Review of the shear-stress transport turbulence model experience from an industrial perspective, *International Journal of Computational Fluid Dynamics*, **23**(4), 305–316.

Menter F. R., Kuntz M., Langtry R. (2003) Ten years of industrial experience with the SST turbulence model, *Turbulence, heat and mass transfer*, **4** (1), 625–632.

Mohanty P. K., Khatua K. K. (2014) Estimation of discharge and its distribution in compound channels, *Journal of Hydrodynamics*, **26** (1), 144–154.

Penttinen O., Yasari E., Nilsson H. (2011) A pimplefoam tutorial for channel flow, with respect to different LES models, *Practice Periodical on Structural Design and Construction*, **23** (2), 1–23.

Piomelli U. (1993) High Reynolds number calculations using the dynamic subgrid-scale stress model, *Physics of Fluids A: Fluid Dynamics*, **5** (6), 1484–1490.

Rusche H. (2002) Computational Fluid Dynamics of Dispersed Two-Phase Flows at High Phase Fractions, *Ph.D. thesis*, Imperial College, University of London.

Sagaut P. (2006) *Large Eddy Simulation for Incompressible Flows: An Introduction*, Second Edition, Verlag Berlin Heidelberg New York: Springer Science & Business Media.

Shiono K., Rameshwaran P. (2015) Mathematical modeling of Bed shear stress and depth averaged velocity for emergent vegetation on floodplain in compound channel, *E-Proceedings of the 36th IAHR World Congress 28 June –3 July, 2015*, The Hague, the Netherlands.

Versteeg H., Malalasekera W. (2007) *An Introduction to Computional Fluid Dynamics: The Finite Volume Method*, Second Edition, England: Pearson Education Limited.

Warner J. C., Sherwood C. R., Arango H. G., Signell R. P. (2005) Performance of four turbulence closure models implemented using a generic length scale method, *Ocean Modelling*, **8** (1–2), 81–113.

White F. M. (1979) Fluid mechanics, *Google Scholar*, 367–375.

Zahiri A. P., Roohi E. (2019) Anisotropic minimum-dissipation (AMD) subgrid-scale model implemented in OpenFOAM: verification and assessment in single-phase and multi-phase flows, *Computers & Fluids*, **180**, 190–205, https://doi.org/10.1016/j.compfluid.2018.12.011.